Proteomic response of wheat embryos to fosthiazate stress in a protected vegetable soil

Chunyan Yin[1,2], Ying Teng[1,2], Yongming Luo[1,2,3,*], Peter Christie[4]

1. Key Laboratory of Soil Environment and Pollution Remediation, Institute of Soil Science, Chinese Academy of Sciences, Nanjing 210008, China.
E-mail: cyyin@issas.ac.cn
2. Graduate University of Chinese Academy of Sciences, Beijing 100049, China
3. Yantai Institute of Coastal Zone Research, Chinese Academy of Sciences, Yantai 264003, China
4. Agri-Environment Branch, Agri-Food and Biosciences Institute, Newforge Lane, Belfast BT9 5PX, United Kingdom

Abstract

A proteomic analysis of wheat defense response induced by the widely used organophosphorus nematicide fosthiazate is reported. Seed germination and two-dimensional gel electrophoresis (2-DE) experiments were performed using a Chinese wheat cultivar, Zhenmai No. 5. Root and shoot elongation decreased but thiobarbituric acid reactive substances (TBARS) content in embryos increased with increasing pesticide concentration. More than 1000 protein spots were reproducibly detected in each silver-stained gel. Thirty-seven protein spots with at least 2-fold changes were identified using MALDI-TOF MS/MS analysis. Of these, 24 spots were up-regulated and 13 were down-regulated. Proteins identified included some well-known classical stress responsive proteins under abiotic or biotic stresses as well as some unusual responsive proteins. Ten responsive proteins were reported for the first time at the proteomic level, including fatty acyl CoA reductase, dihydrodipicolinate synthase, DEAD-box ATPase-RNA-helicase, fimbriata-like protein, waxy B1, rust resistance kinase Lr10, putative In2.1 protein, retinoblastoma-related protein 1, pollen allergen-like protein and S-adenosyl-L-methionine:phosphoethanolamine N-methyltransferase. The proteins identified were involved in several processes such as metabolism, defense/detoxification, cell structure/cell growth, signal transduction/transcription, photosynthesis and energy. Seven candidate proteins were further analyzed at the mRNA level by RT-PCR to compare transcript and protein accumulation patterns, revealing that not all the genes were correlated well with the protein level. Identification of these responsive proteins may provide new insight into the molecular basis of the fosthiazate-stress response in the early developmental stages of plants and may be useful in stress monitoring or stress-tolerant crop breeding for environmentally friendly agricultural production.

Key words: fosthiazate; proteomic; wheat embryo; stress response; biological indicator

DOI: 10.1016/S1001-0742(11)61013-9

Introduction

Fosthiazate, (RS)-S-sec-butyl-O-ethyl-2-oxo-1,3-thiazolidin-3-ylphosphonothioate, is a relatively new non-fumigant organophosphorus nematicide used for the control of nematodes in a wide range of crops such as bananas, potatoes, wheat and tomatoes (Abd-elgawad and Kabeil, 2010; Guzmangonzalez et al., 1994; Kimpinski et al., 1997; Kimpinski et al., 2005). Studies have shown that fosthiazate exhibits efficacy in field plots similar to other non-fumigant nematicides against a wide range of plant parasitic nematodes (Hafez and Sundararaj, 2006; Kimpinski et al., 1997; Woods et al., 1999). Following the ban on the use of other organophosphorus nematicides with high toxicity and methyl bromide on vegetables due to their adverse effect on the environment and human health, fosthiazate, whose use has been rising exponentially in recent years, is considered to be one of the most efficient nematicides in controlling root-knot nematodes in protected crops (Giannakou et al., 2005). Although fosthiazate has largely controlled root-knot nematodes and increased crop production, its improper use (e.g., high application doses and rates) may represent some environmental risk.

The environmental fate of fosthiazate is influenced by soil physical characteristics. Qin et al. (2004) showed that fosthiazate was more persistent in acidic soils than in neutral or alkaline soils with laboratory half-life values in soils ranging from 0.5 to 1.5 months. Pantelelis et al. (2006) revealed that fosthiazate posed a significant risk for groundwater contamination in acidic soils, especially those with low organic matter content. Kungolos et al. (2009) evaluated the toxic effects of fosthiazate, metalaxyl-M and imidachloprid on *Vibrio fischeri*, *Pseudokirchneriella subcapitata* and *Daphnia magna* and pointed out that fosthiazate exhibited the highest toxicity to the aforementioned organisms. However, little work has been done on the responses of non-target plants to fosthiazate

---

* Corresponding author. E-mail: ymluo@yic.ac.cn

toxicity, particularly at the proteomic level. According to Hashiguchi et al. (2010), screening differentially-expressed stress-tolerant proteins is of significance for tolerant crop breeding due to environmental problems and concerns about food safety.

2-DE is used to investigate differentially-expressed proteins in response to abiotic or biotic stresses such as heavy metals (Ahsan et al., 2007a, 2007c), herbicides (Ahsan et al., 2008; Castro et al., 2005; Lin et al., 2008), flooding (Ahsan et al., 2007b; Kong et al., 2010), salt stress (Du et al., 2010), chilling (Lee et al., 2009), ovine saliva (Fan et al., 2010), *Meloidogyne incognita* (de Deus Barbosa, 2009) and pathogens (Lee, 2006). It is well-documented that the germination process is highly disturbed by heavy metals (Xu et al., 2009), herbicides (Song et al., 2007) and antibiotics (Jin et al., 2010). To date, several proteomic studies have been conducted in germinating seeds (e.g., rice seeds, maize seeds and Arabidopsis seeds) under normal conditions or stressed environments (Ahsan et al., 2007a, 2007c; Gallardo et al., 2001; Lu et al., 2008; Yang et al., 2007). However, no proteomic studies have been undertaken to reveal the proteins regulated by fosthiazate during seed germination. It is necessary to analyze the fosthiazate-induced proteome pattern changes in wheat embryos to understand plant systemic responses.

In the present study, the *in vivo* proteomic changes in wheat embryos exposed to fosthiazate stress were addressed. Compared with previously identified stress-responsive proteins, some proteins identified in response to fosthiazate stress are unusual. These findings may provide a framework for studies on the role of the stress-induced proteins associated with plant fosthiazate tolerance and for the future development of strategies for reducing the risk of toxicity of fosthiazate to crops.

1 Materials and methods

1.1 Treatment and germination assay

Wheat (*Triticum aestivum* L.) cultivar Zhenmai No. 5 and the commercial nematicide fosthiazate (10% GR, Ishihara Sangyo Kaisha Ltd., Osaka, Japan) were used. Uncontaminated soil was collected from the top 20 cm of the soil profile in a protected vegetable field at Shouguang County, Shandong Province, Northeast China. The soil samples were gently crumbled by hand, air-dried at room temperature and sieved through a 2-mm mesh to remove root residues and small stones. Selected soil physicochemical properties were: organic matter 10.6 g/kg, pH (in water) 7.4, total N 0.60 g/kg, total P 0.72 g/kg and total K 16.82 g/kg. Aliquots of soil were mixed thoroughly with fosthiazate at concentrations of 0, 12.5, 50, 100 and 200 mg/kg soil. The application rate 12.5 mg/kg is within the recommended application rate (10–13.3 mg/kg). Distilled water was added to adjust the amended soil to 60% of field capacity. The spiked soil was allowed to stand for 24 hr at 25°C in the dark to equilibrate. The germination assay was conducted according to Wang and Zhou (2005). Wheat seeds were surface-sterilized with 10% (*V/V*) sodium hypochlorite solution (Sinopharm Chemical Reagent Co. Ltd., China) for 10 min followed by a thorough washing in distilled water. Twenty-five seeds were placed in each Petri dish (90 mm in diameter) containing 40 g prepared soil. The seeds germinated for 60 hr (control root length > 2 mm) in the dark at 25°C and 50% humidity. The shoot and root lengths were recorded. The experiment was repeated at least 3 times.

1.2 Measurement of Thiobarbituric Acid Reactive Substances (TBARS) content

Accumulation of lipid peroxides in tissues was determined in terms of TBARS based on the method of Song et al. (2007).

1.3 Protein extraction

Proteins were extracted from germinating seeds after 60 hr exposure using the acetone-precipitation method according to Fan et al. (2010) with some modification. After germination, the embryos were separated from the endosperms using a surgical blade and immediately frozen in liquid nitrogen. About 1.0 g (fresh weight) embryos were ground in a mortar with liquid nitrogen to a fine powder, suspended in 10 mL newly prepared extraction buffer containing 62.5 mmol/L Tris-HCL (pH 7.5), 10% (*V/V*) glycerol, 0.5% (*W/V*) SDS, 1% (*W/V*) polyvinyl polypyrrolidone and 5% (*V/V*) β-mercaptoethanol and kept at 4°C for 1 hr, followed by centrifugation at 12,000 ×*g* and 4°C for 20 min. The supernatant was precipitated with ice cold acetone (3 times the volume) at –20°C for 2 hr and then centrifuged at 5000 ×*g* and 4°C for 10 min. The acetone-precipitated proteins were air-dried at 4°C for 5 min and stored at –80°C prior to use. Protein content was measured according to Bradford (1976).

All the other chemicals used in the protein preparation and 2-DE were purchased from Sinopharm Chemical Reagent Co. Ltd., China and were of analytical grade.

1.4 Isoelectric focusing and SDS-PAGE

The acetone-precipitated samples were purified with a 2D-clean-up kit (GE Healthcare Biosciences, Pittsburgh, PA, USA) and redissolved with a rehydration buffer (7 mol/L urea, 2 mol/L thiourea, 4% (*W/V*) CHAPS, 65 mmol/L DTT, 0.2% (*W/V*) Biolyte (Bio-Rad, Hercules, CA, USA)). The protein content was then measured according to Bradford (1976).

Isoelectric focusing of acetone-precipitated protein was performed as described in the literature (Tang et al., 2010). Each sample of 350 μL containing 100 μg of protein was applied to a dry IPG strip pH 4–7 (17 cm, Bio-Rad, Hercules, USA) during the passive rehydration step (12 hr), followed by focusing for 56,000 V·hr using a Protean IEF Cell (Bio-Rad, Hercules, USA) at 20°C. After isoelectric focusing, the IPG strips were equilibrated for 15 min in equilibrated buffer (6 mol/L urea, 2% (*W/V*) SDS, 0.375 mol/L Tris-HCl (pH 8.8), 20% (*V/V*) glycerol) containing 20 mg/mL DTT, followed by 15 min in equilibrated buffer containing 25 mg/mL iodoacetamide. SDS-PAGE in the second dimension was carried using a 10% polyacrylamide

gel. The 2-DE gels were silver stained: The gels were stabilized in ethanol: acetic acid: deionized water (5:1:4, $V/V/V$) for 2.5 hr, and then transferred into acetic acid containing sodium acetic acid and sodium thiosulfate on a rotator at 100 r/min for 30 min. The gels were washed with deionized water for 10 min and the process was repeated 3 times. Then the gels were stained with silver nitrate in the dark for 20 min. After staining, the gels were washed and transferred into anhydrous sodium carbonate solution for about 5 min. Finally, the gels were put into Na_2EDTA solution to stop the reaction and imaged. Three independent replicates were performed for each sample. The experiments were performed at least 3 times.

1.5 Protein imaging

Silver-stained gels were used for image and data analysis. The intensities of the protein spots from excess fosthiazate-treated samples were recorded using a high-resolution scanner (GS-800 Calibrated Imaging Densitometer, Bio-Rad, USA). The intensity of each protein spot was normalized relative to the total abundance of all valid spots. Spots were detected and quantified with Bio-Rad PDQuest software (V8.0, Bio-Rad, USA). Only spots that exhibited at least two-fold intensity changes between control and treated samples were considered to be differentially-expressed proteins.

1.6 In-gel digestion and MALDI-TOF MS-MS analysis

Silver-stained protein spots were identified as described by Requejo and Tena (2005) with some modification. Protein spots with at least 2-fold increase/decrease were excised manually from the silver-stained gel, dehydrated in acetonitrile (ACN), reduced with 10 mmol/L DTT in 25 mmol/L NH_4HCO_3 and alkylated with 55 mmol/L iodoacetamide in 25 mmol/L NH_4HCO_3. Gel pieces were washed thoroughly with 25 mmol/L NH_4HCO_3, 50% (V/V) ACN and 100% (V/V) ACN and then dried. Dried gel pieces were digested with trypsin (Promega, Madison, USA) solution (10 ng/mL in 25 mmol/L NH_4HCO_3) at 47°C for 30 min and incubated at 37°C for 12 hr. Trifluoroacetic acid (TFA) was added to a final concentration of 0.1% (V/V) to stop the digestive reaction. All samples were analyzed over the mass range (m/z 700–4000) in the positive-ion reflection mode, on a TOF Ultraflex II mass spectrometer (Bruker Daltonics, USA). The mass spectra obtained were processed by FlexAnalysis v2.4 software

(Bruker Daltonics, USA) with the following settings: peak detection algorithm set at SNAP (Sort Neaten Assign and Place), S/N threshold at 3, and Quality Factor Threshold at 50. Then the resulting peptide mass was used to search Swiss-Prot and TrEMBL databases. The following parameters were used as criteria in the search: significant protein MOWSE score at $p < 0.05$; minimum mass accuracy at 100 ppm; trypsin as enzyme; one missed cleavage site allowed; cysteine carbamidomethylation, acrylamide-modified cysteine, methionine oxidation, similarity of isoelectric point, and relative molecular mass specified; the minimum sequence coverage at 15%.

Samples identified by PMF were automatically submitted to MS/MS analysis. Three of the strongest peaks of the TOF spectra per sample were chosen for MS/MS analysis. For MS/MS spectra searching, the spectra were used to search the Swiss-Prot 50.1 and TrEMBL 34.0 databases (downloaded locally) automatically using MASCOT (V2.4). Search parameters for MS/MS data included 100 ppm for the precursor ion and 0.3 Da for the fragment ions. Cleavage specificity and covalent modifications were considered as described above and the score was higher than the minimal significant ($p < 0.05$) individual ion score. All significant MS/MS identifications by MASCOT were manually verified for spectral quality and matching y and b ion series. When there were multiple entries corresponding to slightly different sequences, only the database entry with the most matching peptides was included.

1.7 Real-time quantitative RT-PCR

Total RNA was isolated from frozen embryos by the SV Total RNA Isolation System Kit (Promega, Madison, WI, USA). For all samples, first strand cDNA was synthesized from total RNA using SuperScript II RNase H reverse transcriptase (Invitrogen, Carsbad, USA) and an oligo(dT) adaptor primer (5′-GACTCGAGTCGATCGA(-dT)17-30-3′) as described in the manufacturer's protocol. Primers were designed from the peptide sequences obtained after MS/MS analysis. The uniqueness of the primers was validated by PCR reaction, DNA sequencing and sequence comparing. Gene-specific primers used for PCR are provided in Table 1. The wheat elongation factor TaEF-1α gene (GenBank ID: Q03033) was used as the internal reference for the RT-PCR. RT-PCR was carried out on the ABI PRISM 7300 Real-time PCR system with the SYBR® Premix Ex Taq™ (Takara Bio Inc., Shiga, Japan) according-

Table 1   Primer sequences used for real-time RT-PCR

Spot ID	Protein name	Forward primer (5′–3′)	Reverse primer (5′–3′)
1	Ca^{2+} binding protein cbp1	TCAGTTCGCAAAGCATCAAC	GCCTTTAGCGAATCTTGCAC
8	Glutathione S-transferase tau class	AGATACCCGTGCTCATCCAC	CCAGCTTGTCGTCAACGTAA
12	Phosphoglucomutase	CCGGCCTCCGCAAGAAGGTT	AAATAGCGCCCATCGCCGGA
28	Putative In2.1 protein	GCACTGCTTCCTCAAGATCC	GTCACGTACGCAATGTCCAC
30	Retinoblastoma-related protein	TGCTCGGATGTTTCAGAGTG	ACTGCCAAGCAAACTGTCCT
34	S-adenosyl-L-methionine: phosphoethanolamine N-methyltransferase	CCGCGGAAATCGCTGCCAAC	GCGCGGGAGTCGAGCATCAT
35	ATP synthase beta subunit	ACACTGCCCGTGGTGTCCAGA	ACGCGTGCTCCGAGATGTCG
	TaEF-1α gene	TGGTGTCATCAAGCCTGGTATGGT	ACTCATGGTGCATCTCAACGGACT

TaEF-1α gene: the internal reference for RT-PCR analysis (GenBank ID: Q03033).

ing to the manufacturer's protocol. Three templates were prepared for each sample, and each template amplification was performed 3 times.

1.8 Statistical analysis

All data were presented as mean values ± standard deviation (SD) of triplicates. Statistical analyses were performed by SPSS (13.0) for windows. One way ANOVA with the Least Significant Difference (LSD) test was used to assess differences among means at 0.05 and 0.01 levels.

2 Results and discussion

2.1 Toxic effects of fosthiazate on wheat seedlings

As shown in Fig. 1, there was a significant linear correlation between the inhibitory rate of root and shoot elongation and the tested concentration of fosthiazate ($p < 0.01$). The inhibitory rate of root and shoot elongation increased with increasing concentration of fosthiazate in the tested soil. According to the corresponding regression equations based on the inhibition of root and shoot elongation, the EC_{50} values of fosthiazate for root and shoot were 141 and 204 mg/kg, respectively. The EC_{50} of root was about ten times the normal application dose.

Lipid peroxidation can be determined by the formation of TBARS as the decomposition products of the membrane lipid. As shown in Fig. 2, there was no significant difference for the TBARS formation between control and lower treatment concentrations (e.g., 12.5 and 50 mg/kg). But a substantial accumulation of TBARS was observed in organisms subjected to 200 mg/kg fosthiazate ($p < 0.05$). As addressed by Ahsan et al. (2007a) and Song et al. (2007), TBARS formation in plants exposed to environmental stress has often been considered to be a reliable indicator of cellular ROS generation. Therefore, in the present study, the accumulation of TBARS might indicate that a large quantity of ROS is generated by fosthiazate stress. To gain a better understanding of fosthiazate stress-responsive proteins, the organisms treated with 200 mg/kg fosthiazate were chosen.
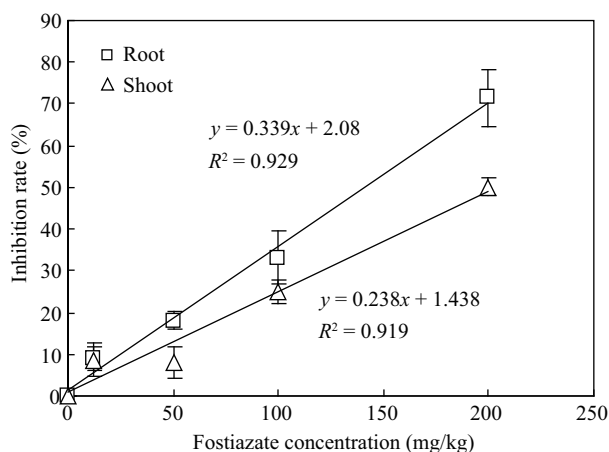

Fig. 1 Inhibition effects of fosthiazate on wheat root and shoot elongation. The regression equations of root and shoot to fosthiazate were obtained by SPSS ($p < 0.01$). Data are mean values ± SD of triplicates.
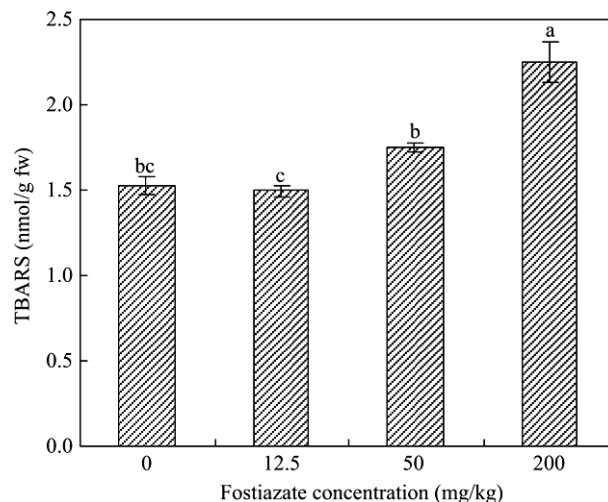

Fig. 2 Fosthiazate-induced TBARS formation in embryos of germinating wheat seeds. The data were expressed on fresh weight (fw) basis. Data are mean values ± SD of triplicates. The different letters indicate significant differences at $p < 0.05$.

2.2 Proteome changes in wheat embryos exposed to fosthiazate stress and MALDI-TOF MS/MS analysis

Proteome patterns of wheat embryo after short-term exposure to excess fosthiazate (200 mg/kg) were detected by 2-DE. After 60 hr exposure, embryos were harvested from germinating wheat seeds for total protein extraction and 2-DE. With the use of PDQuest software, more than 1000 silver-stained protein spots were reproducibly detected through three independent replicates on each 2-D gel for control and treatment (Supporting materials). Among these, a total of 50 notably differentially ($p < 0.01$) accumulated and reproducible protein spots were detected.

Out of these differentially-expressed protein spots, 37 protein spots with significant change (at least 2-fold increase/decrease) were excised from the gels and digested with trypsin and the peptides were identified by MALDI-TOF MS/MS (Fig. 3). The database search results are listed in Table 2. In response to fosthiazate, 24 out of 37 identified proteins spots were up-regulated and 13 protein spots were down-regulated, suggesting that wheat actively responds to fosthiazate stress. Among 37 spots, there were eight protein spots (spot 11, 16, 28, 31, 33, 34, 35 and 36) newly induced and one protein spot (spot 12) disappeared in fosthiazate-stressed organisms.

2.3 Defense response of wheat embryos to fosthiazate stress

The identified stress-responsive proteins were further categorized on the basis of their putative functions, and mainly fell into six different functional classes: (1) signal transduction and transcription, (2) metabolism, (3) defense and detoxification, (4) cell structure and growth, (5) photosynthesis and energy, (6) miscellaneous (Fig. 4). Spot 23 was identified as putative protein. It was up-regulated nearly 6-fold in the fosthiazate-stressed embryos (Table 2). However, its specific role in response to fosthiazate remains unclear and requires future investigation. Proteins involved in metabolism and defense/detoxification

Table 2 Fosthiazate-induced differentially-expressed proteins in wheat embryos identified by MALDI-TOF MS/MS analysis

Spot ID	Protein description	Organisms	NCBI accession No.	Theoretical Mr (kDa)/pI	MP	MOWSE score	SC (%)	Fold change
Signal transduction and transcription								
1↓	Ca²⁺ binding protein cbp1	*Triticum aestivum*	gi|58198731	86.8/5.7	39	385	59	<4
3↓	Rust resistance kinase Lr10	*Triticum aestivum*	gi|1680686	71.0/6.3	28	443	52	<16
5↑	Protein kinase, putative, expressed	*Triticum aestivum*	gi|300681429	58.8/6.5	28	469	52	>2.5
25↑	DEAD-box ATPase-RNA-helicase	*Triticum aestivum*	gi|68037499	41.4/9.5	37	518	60	>8
29↑	Fimbriata-like protein	*Triticum aestivum*	gi|86439727	42.6/8.6	26	365	74	>2.4
Metabolism								
6↓	Phosphoglucomutase	*Triticum aestivum*	gi|18076790	62.8/5.7	27	585	50	<4
7↓	Phosphoglucomutase	*Triticum aestivum*	gi|18076790	62.8/5.7	21	400	34	<2.7
12↓	Phosphoglucomutase	*Triticum aestivum*	gi|18076790	62.8/5.7	17	199	31	–
14↑	Dihydrodipicolinate synthase 2, chloroplastic	*Triticum aestivum*	gi|118237	40.9/6.8	36	573	71	>5.4
16↑	Fatty acyl CoA reductase	*Triticum aestivum*	gi|22003082	57.5/8.8	28	481	56	New
17↑	Glycosyltransferase	*Triticum aestivum*	gi|56409846	53.0/6.1	37	754	48	>4
20↓	Glutamine synthetase isoform GSr1	*Triticum aestivum*	gi|40317416	38.7/5.4	12	123	35	<2.9
21↑	Waxy B1	*Triticum aestivum*	gi|310619518	63.3/8.5	37	470	70	>5.8
22↑	Starch synthase	*Triticum aestivum*	gi|1620660	55.7/6.2	26	321	59	>4
27↑	Chloroplast fructose-bisphosphate aldolase	*Triticum aestivum*	gi|223018643	42.0/6.0	32	581	52	>9
32↓	Cytosolic aconitase	*Triticum aestivum*	gi|290783890	50.2/5.8	28	586	54	<2.5
Defense and detoxification								
2↓	1-Cys peroxiredoxin	*Triticum turgidum* subsp. *durum*	gi|12247762	23.9/6.3	21	347	63	<2.6
8↑	Glutathione S-transferase tau class	*Triticum aestivum*	gi|21730248	24.8/5.6	18	311	49	>5
9↑	Putative In2.1 protein	*Triticum aestivum*	gi|3393062	27.1/5.4	35	649	84	>16
10↑	Hypersensitive response protein	*Triticum aestivum*	gi|146231063	31.3/5.3	41	733	73	>6
13↓	Glutathione-S-transferase	*Triticum aestivum*	gi|21956482	24.8/5.5	33	606	78	<2.9
18↓	Heat shock protein Hsp26	*Triticum aestivum*	gi|4028571	26.6/7.9	24	477	82	<2.4
19↑	Putative In2.1 protein	*Triticum aestivum*	gi|3393062	27.1/5.4	11	206	33	>2.6
26↑	Hypersensitive response protein	*Triticum aestivum*	gi|146231063	31.3/5.3	33	575	70	>3.6
28↑	Putative In2.1 protein	*Triticum aestivum*	gi|3393062	27.1/5.4	20	407	61	New
31↑	Glutathione transferase F3	*Triticum aestivum*	gi|23504741	24.5/5.3	25	442	45	New
34↑	S-adenosyl-L-methionine: phosphoethanolamine N-methyltransferase	*Triticum aestivum*	gi|259018725	57.0/5.3	30	465	55	New
36↑	Ascorbate peroxidase	*Triticum aestivum*	gi|226897533	26.7/5.5	18	340	67	New
Cell structure and growth								
15↓	Tubulin beta-5 chain	*Zea mays*	gi|162462765	50.7/4.8	19	294	44	<3
24↑	Putative cellulose synthase	*Triticum aestivum*	gi|40363755	120.9/7.5	42	523	48	>6
30↑	Retinoblastoma-related protein 1	*Triticum aestivum*	gi|254789784	106.0/8.9	35	611	35	>2
33↑	Pollen allergen-like protein	*Triticum aestivum*	gi|972513	13.3/9.3	21	329	98	New
37↓	Cyclin-dependent kinase-like B2	*Triticum aestivum*	gi|226359369	37.0/9.0	19	324	63	<2.9
Photosynthesis and energy								
4↓	Vacuolar proton-ATPase subunit A	*Triticum aestivum*	gi|90025017	68.4/5.2	27	523	46	<2.6
11↑	33 kDa subunit of oxygen evolving system of photosystem II, precursor	*Triticum aestivum*	gi|131388	34.7/8.7	15	382	26	New
35↑	ATP synthase beta subunit	*Triticum aestivum*	gi|525291	59.2/5.6	29	596	49	New
Miscellaneous								
23↑	Putative protein	*Triticum aestivum*	gi|255091050	52.3/5.8	24	328	52	>6

↑: up-regulated proteins; ↓: down-regulated proteins; Mr: relative molecular mass; pI: isoelectric point; MP: number of matched peptides; SC: sequence coverage; fold change: protein fold increased (>) or decreased (<) compared to the control; New: newly induced; –: disappeared.

were found to predominate (Fig. 4). These results show that wheat embryos recognize fosthiazate stress, regulate metabolic patterns and adjust cell structure and function to adapt to the stress.

2.3.1 Metabolism-related proteins

Metabolism-related proteins were found to be significantly up- or down-regulated during germination in wheat, as detected in tomato, rice and cucumber (Ahsan et al., 2007b, 2007c; Du et al., 2010). In the present study we detected differential expression of proteins involved in carbohydrate, fatty acid and amino acid metabolism.

Among these, chloroplast fructose-bisphosphate al-dolase, (FBP aldolase, spot 27) related to glycolysis, was predominantly expressed during seed germination under fosthiazate stress. Up-regulation of FBP aldolase during germination might indicate that seeds need more energy to cope with fosthiazate stress. However, FBP aldolase was observed to decrease under salt stress in cucumber and flooding stress in wheat (Du et al., 2010; Kong et al., 2010). Another protein, cytosolic aconitase (spot 32) related to the citrate cycle, decreased significantly compared to the control. This was similar to Du et al. (2010), who found that enzymes involved in the citrate cycle (pyruvate dehydrogenase E1, malate dehydrogenase) were down-regulated in cucumber subjected to salt stress, suggesting carbohydrate metabolism and energy consumption reduction. Thus, glycolysis may be the main energy
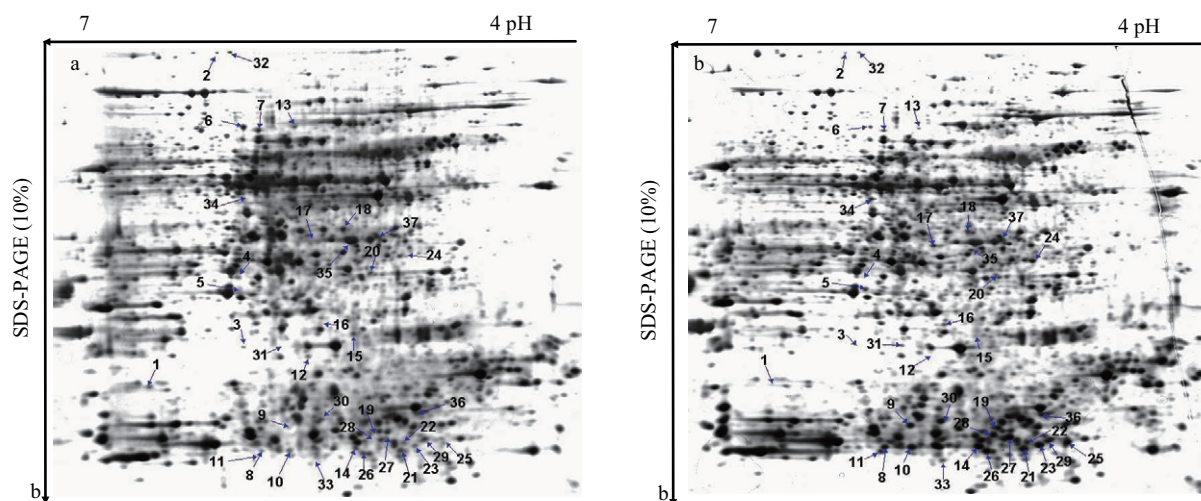
Fig. 3 The 2-DE protein profiles of wheat embryos subjected to fosthiazate stress. Proteins were extracted from the wheat embryos in the absence (a) and presence (b) of 200 mg/kg fosthiazate for 60 hr and separated by 2D-PAGE. The spots were visualized by silver staining. The identified and differentially-expressed protein spots in response to fosthiazate stress are numbered and indicated by arrows.
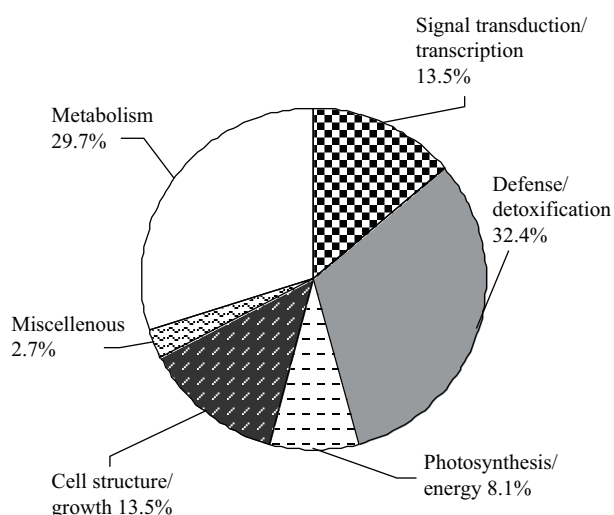

Fig. 4 Functional categorization of proteins identified by 2-DE. Proteins were classified using the NCBI database.

supply in germinating wheat seeds under fosthiazate stress.

In our study three spots (6, 7 and 12) were identified as phosphoglucomutase, and spot 12 disappeared in fosthiazate-stressed organisms. Phosphoglucomutase can determine the pathways of starch synthesis or carbohydrate decomposition (Davies, 2003). Down-regulation of such an enzyme in fosthiazate stress response might indicate starch conservation. It has also been reported that phosphoglucomutase is up-regulated in rice under Cd stress (Kim and Lee, 2009). Another two enzymes correlated with starch synthesis were involved in response to fosthiazate stress. Spots 21 and 22 were matched with starch synthase and waxy B1, respectively. The expression levels of these two enzymes were both over 4-fold higher in fosthiazate-stressed embryos, further suggesting that starch synthesis (not hydrolysis) is usually involved in response to fosthiazate stress at the germination stage. Similar results were reported in rice, that AGPP, an enzyme catalyzing starch biosynthesis, was up-regulated by ovine saliva stress (Fan et al., 2010; Yan et al., 2005) and the activity of amylase, a hydrolase of starch, was decreased significantly

by treatment with copper (Ahsan et al., 2007a). Our results imply that wheat embryos may fail to mobilize reserves under fosthiazate stress and maintain enough energy in the form of starch to prepare for undergoing fosthiazate stress. This may be the first report of waxy B1 at the proteomic level.

A prominent alteration of dihydrodipicolinate synthase 2 (DHDPS, spot 14) was observed for fosthiazate treatment. An approximately 5-fold accumulation occurred in treated embryos compared to the control. DHDPS can be used as a source of energy and substrates for carbohydrate metabolism. Decreased induction of glutamine synthetase isoform GSr1 (spot 20) was observed. Glutamine synthetase (GS) can be differentially expressed under various stresses (Ahsan et al., 2008, 2010; Alam et al., 2010; Yan et al., 2005) and it was reported that GS could enhance stress tolerance (Teixeira et al., 2006).

As identified in our study, fatty acyl CoA reductase (spot 16) was newly induced by fosthiazate stress, which can contribute to NADPH formation used to produce long-chain fatty acid. Accumulation of fatty acyl CoA reductase may be ascribed to suppression of the citrate cycle due to down-regulation of aconitase, and may suggest that wheat embryos obtain more energy through long-chain fatty acid oxidation to enhance fosthiazate tolerance. In summary, wheat embryos adjusted the metabolic pathway to improve fosthiazate tolerance, and some unusual stress-responsive proteins were induced (e.g., waxy B1, DHDPS and fatty acyl CoA reductase).

2.3.2 Defense/detoxification-related proteins

Many stress- and defense-related proteins including ascorbate peroxidase (APx, spot 36), 1-cys peroxiredoxin (spot 2), glutathione S-transferase (GSTs, spots 8, 13 and 31), S-adenosyl-L-methionine:phosphoethanolamine N-methyltransferase (PEAMT, spot 34), putative In2.1 protein (spots 9, 19 and 28), hypersensitive response protein (spots 10 and 26) and heat shock protein Hsp26 (spot 18) were differentially expressed under fosthiazate stress. Putative In2.1 protein and PEAMT are also unusual

stress-responsive proteins.

As expected, APx, GSTs, and 1-cys peroxiredoxin, related to antioxidant enzymes to maintain intracellular ROS balances, were differentially detected (Cummins et al., 1999; Qureshi et al., 2007). As indicated in Table 2, APx was newly produced in fosthiazate-stressed embryos, suggesting that the embryos suffered from ROS toxicity. In the current study the fact that GSTs proteins (spots 8, 13 and 31) with similar relative molecular mass and isoelectric point were so scattered on the gels may be mainly due to the presence of different isoforms or post-translational modifications (Ahsan et al., 2007c, 2008; Kong et al., 2010). Because of differential expression of GSTs under fosthiazate stress, the mechanisms of GSTs in fosthiazate-stress tolerance are unclear and complex. Nevertheless, the increased induction of a tau class GST by fosthiazate stress may be responsible for fosthiazate detoxification owing to the classic xenobiotic detoxification function (Lin et al., 2008). The 1-cys peroxiredoxin expression level declined nearly 2.6-fold compared to the control. This enzyme also regulated phospholipid turnover, which could result in suppression of wheat root elongation (Chen et al., 2000).

There exists a strong correlation between heat shock proteins (Hsps) accumulation and plant tolerance to stress (Sun et al., 2002; Wang et al., 2004). Of the Hsps, the small heat shock proteins (sHsps) are the most prevalent in plants and mainly responsible for stabilizing and preventing aggregation of proteins (Lee and Vierling, 2000). In our study the expression level of Hsp26 decreased slightly, which might lead to protein denaturation and inhibition of wheat seedling elongation.

S-adenosyl-L-methionine:phosphoethanolamine N-methyltransferase (PEAMT, spot 34), an enzyme related to membrane phospholipid phosphatidylcholine synthesis (Palavalli et al., 2006), was newly induced during fosthiazate treatment. Studies have indicated that PEAMT can enhance plant tolerance to environmental stress (Mou et al., 2002). Thus, we can conclude that up-regulation of PEAMT in response to fosthiazate might confer wheat seed embryos resistance to fosthiazate stress. Putative In2.1 protein (spots 9, 19 and 28) accumulated substantially in fosthiazate-treated embryos, with one protein spot newly induced. Recently, Riechers et al. (2010) indicated that putative In2.1 protein could activate plant defense gene expression and detoxification. Putative In2.1 protein is another unusual protein in fosthiazate stress response.

2.3.3 Cell structure and growth-related proteins

As excess fosthiazate significantly inhibited root and shoot elongation, a group of differentially-regulated proteins related to cell structure and cell division/extension were identified (Table 2).

Tubulin beta-5 chain (spot 22) comprises the major subunit of microtubules and participates in plant cell shape formation and plant development (Radchuk et al., 2007; Schröder et al., 2001). In our study tubulin beta-5 chain was down-regulated during fosthiazate exposure. Hence, fosthiazate may interrupt the activity of cell micro-

tubules. Glycosylthansferase and cellulose synthase (spot 24), which play a part in the synthesis of cell walls (Fanous et al., 2007), accumulated under fosthiazate stress. Thus, we can infer that excess fosthiazate might damage cell membranes and activate glycosyltransferase and cellulose synthase to strengthen the cell walls. In plants, cyclin-dependent kinases (CDKs) (spot 37) are encoded by several gene families and play important roles in cell cycle progression (Mironov and Inze, 1999). Schuppler et al. (1998) suggested that water stress inhibited the growth of wheat leaf basal meristem due to inhibition of CDKA1 activity. In the present study a reduced expression level of CDKB2 was observed under fosthiazate exposure. Thus, suppression of root and shoot elongation under fosthiazate stress can be ascribed to inhibition of CDKB2. Retinoblastoma-related protein 1 (NtRBR1, spot 30), controlling the progression of the cell cycle from G1 to S phase (Hirano et al., 2008), accumulated in treated embryos. Pollen allergen-like protein (spot 33), a newly-induced protein under fosthiazate treatment, was identified as a homolog of expansin, which can mediate cell wall extension (Shcherban et al., 1995). To our knowledge, this is the first evidence for the accumulation of NtRBR1 and pollen allergen-like protein in the stress response process. In summary, these results suggest that under fosthiazate stress the organisms may adjust cell skeleton, cell division and cell wall extension to survive such serious environmental challenges.

2.3.4 Photosynthesis- and energy-related proteins

In the present study one protein related to photosynthesis (33 kDa subunit of oxygen evolving system of photosystem II, precursor, spot 15) newly accumulated in fosthiazate-stressed wheat embryos. It has been reported that this enzyme is greatly induced under stresses (Ahsan et al., 2008; Castro et al., 2005). Induction of this enzyme in response to fosthiazate may indicate that wheat embryos are going to obtain energy and substrates for stress defense and for later self development through photosynthesis due to inhibition of the citrate cycle at the onset of germination.

Two differentially-expressed energy-related proteins were identified as vacuolar proton-ATPase subunit A (spot 4) and ATP synthase beta subunit (spot 35), respectively. As suggested by Du et al. (2010), up-regulation of vacuolar proton-ATPase subunit A was associated with osmotic adjustment. In our study the expression of this enzyme was more than halved compared to the untreated embryos, indicating that fosthiazate might cause osmotic stress to wheat at the germination stage. ATP synthase beta subunit was newly induced, which indicates plants need a large amount of energy to cope with fosthiazate stress and enhance defense ability. This enzyme was also reported to be down-regulated when plants were subjected to salt stress or ovine saliva (Du et al., 2010; Fan et al., 2010).

2.3.5 Signal transduction and transcription-related proteins

A group of proteins associated with the signal transduction regulation process were differentially expressed in re-

sponse to fosthiazate. This group comprised Ca^{2+} binding protein cbp1 (spot 1), rust resistance kinase Lr10 (spot 3), protein kinase (spot 5), DEAD-box ATPase-RNA-helicase (spot 25) and fimbriata-like protein (spot 29).

Down-regulation of Ca^{2+} binding protein cbp1 (spot 1) was detected in our study. Similar to the findings of Squier (2006), down-regulation of Ca^{2+} binding protein cbp1 might be a signal to slow down the metabolism rate and enhance tolerance ability, which can become a unique defense mechanism of wheat embryos against fosthiazate stress.

Rust resistance kinase Lr10 (spot 3) and putative protein kinase (spot 5) both belong to the protein kinase superfamily. They both have protein serine/threonine kinase activity. Ge et al. (2007) reported that excess expression of the serine/threonine kinase gene (TaSTK) enhanced salt tolerance. Differential regulation of the two protein kinases in signaling transduction might suggest fosthiazate tolerance enhancement. To our knowledge, rust resistance kinase Lr10 is an unusual responsive protein under fosthiazate stress.

The abundance of spot 25 increased greatly in fosthiazate-treated embryos and it was identified as DEAD-box ATPase-RNA-helicase, which belongs to the DEAD-box helicase family (Okanami et al., 1998). It was reported that over-expressing OsBIRH1, which encodes a DEAD-box RNA helicase, increased tolerance to oxidative stress and pathogen infection (Li et al., 2008). Also, Fan et al. (2010) found that up-regulation of BAT1, a member of the DEAD-box helicase, in rice subjected to ovine saliva enhanced defense ability. Similarly, increased expression of DEAD-box ATPase-RNA-helicase by fosthiazate was involved in the stress response and may assist in the acquisition of fosthiazate tolerance. This enzyme is also an unusual stress-responsive protein.

The expression level of fimbriata-like protein (spot 29) in treated embryos was 2.6 times higher than in untreated embryos. It belongs to F-box protein, which can degrade targeting proteins through activated ubiquitin in plants (Kipreos and Pagano, 2000). Similarly, in the current study the up-regulation of such an F-box protein might indicate involvement in degradation of targeting proteins which down-regulate the fosthiazate response. Expression of the F-box protein has also been reported to be stimulated by water stress (Alam et al., 2010). As far as we know, fimbriata-like protein is also an unusual stress-responsive protein that was identified in the present study and this may be the first evidence for accumulation of such a protein in the stress response pathway.

2.4 Changes of gene regulation at mRNA level in response to fosthiazate stress

Among all the identified proteins, five were randomly selected to investigate their expression patterns at the transcript level (Fig. 5). Total RNA was extracted from the embryos in the absence and presence of fosthiazate (200 mg/kg), followed by real time RT-PCR. Results showed that transcription of putative In2.1 protein and glutathione S-transferase tau class was also induced by fosthiazate

stress (Fig. 5). As up-regulation of such proteins related to defense and detoxification at the mRNA level, we can conclude that wheat embryos enhance fosthiazate stress tolerance by regulating gene expression. Due to its new induction, the unusual response protein – putative In2.1 protein also has potential to serve as a biomarker in fosthiazate stress monitoring. However, in the future we will still need to study the concentration-dependent protein expression profiles of wheat embryos stressed by fosthiazate to verify the possibility of this novel protein to be an indicator of fosthiazate stress in the plant. Other proteins, including Ca^{2+} binding protein cbp1, phosphoglucomutase, retinoblastoma-related protein 1, PEAMT and ATP synthase beta subunit did not show the same expression patterns at the mRNA level as at the proteomic level. Nevertheless, our results are in accord with several studies revealing large numbers of genes without good correlation between the mRNA and protein levels (Du et al., 2010; Lin et al., 2008). This phenomenon could ascribe to mRNA instability, translational regulation, post-translational modified, or protein degradation (Fan et al., 2010). Besides, RT-PCR cannot differentiate the isoforms of proteins and identify the specific ones especially when the protein belongs to a multigene family (Du et al., 2010). This becomes one limitation for RT-PCR to compare the transcript and protein accumulation.

3 Conclusions

Cereal embryos are considered to be a model system to study stress tolerance (Irar et al., 2010). To the best of our knowledge this is the first proteomic analysis of the extensive changes in wheat embryos after exposure to excess fosthiazate. Fosthiazate stress induced proteome pattern changes in wheat embryos. A total of 37 proteins identified by MALDI TOF MS/MS analysis were differentially expressed in response to fosthiazate stress. These proteins were involved in several processes that might work cooperatively to establish a new homeostasis under fosthiazate stress. Firstly, via signal transduction wheat embryos restrict cell growth, slow down the metabolism rate and reserve large quantities of carbohydrate resources for cell skeleton reconstruction and extension. Secondly, ROS formation is the main form of toxicity during fosthiazate stress, and wheat embryos enhance their defense/detoxification ability by regulating gene expression. Ultimately, through β-oxidation of long chain fatty acids, wheat embryos obtain a large quantity of energy to cope with fosthiazate stress and for subsequent development. Here we identify ten unusual responsive proteins such as fatty acyl CoA reductase, DHDPS, DEAD-box ATPase-RNA-helicase, fimbriata-like protein, waxy B1, rust resistance kinase Lr10, putative In2.1 protein, retinoblastoma-related protein 1, PEAMT and pollen allergen-like protein. Four unusual responsive proteins (fatty acyl CoA reductase, putative In2.1 protein, pollen allergen-like protein and PEAMT) were also newly induced in response to fosthiazate stress. Thus, they might have the potential to function as biomarkers in order to
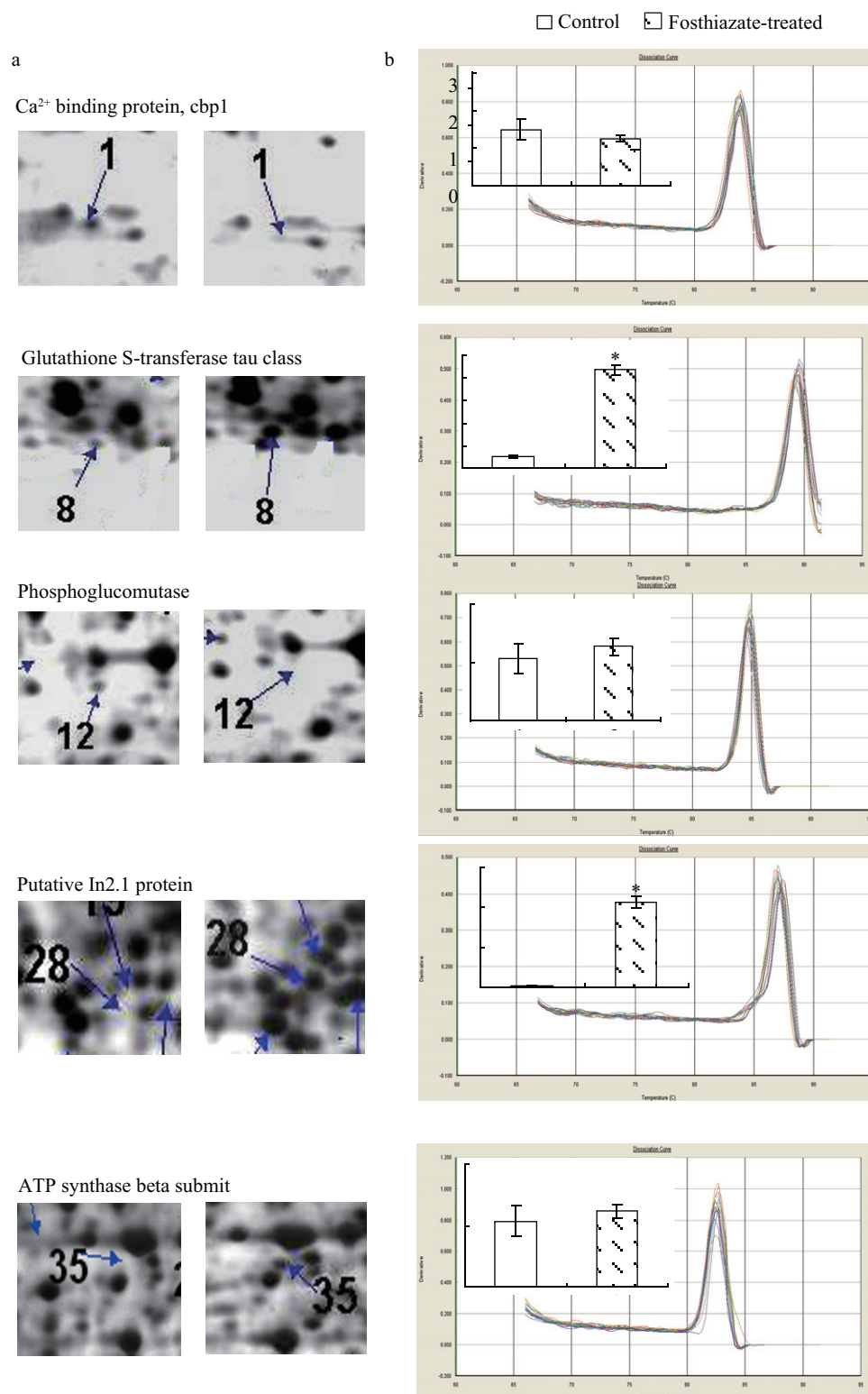
Fig. 5 Real-time RT-PCR analysis of five candidate proteins in wheat embryos subjected to fosthiazate stress. (a) magnified views of the candidate protein spots; (b) the corresponding SYBR fluorescence dissociation curves embedded with the histograms of mRNA expression levels of the protein spots. * Significant differences at $p < 0.05$.

detect fosthiazate stress in the plants. This study provides basic data and a framework for further investigations.

Supporting materials

Supporting data associated with this article can be found in the online version.

References

Abd-elgawad M M M, Kabeil S S A, 2010. Management of the root-knot nematode, *Meloidogyne incognita* on tomato in Egypt. *Plant Pathology*, 6(8): 256–262.

Ahsan N, Lee D G, Lee S H, Kang K Y, Lee J J, Kim P J et al., 2007a. Excess copper induced physiological and proteomic changes in germinating rice seeds. *Chemosphere*, 67(6): 1182–1193.

Ahsan N, Lee D G, Lee S H, Lee K W, Bahk J D, Lee B H, 2007b. A proteomic screen and identification of waterlogging-regulated proteins in tomato roots. *Plant Soil*, 295(1-2): 37–51.

Ahsan N, Lee S H, Lee D G, Lee H, Lee S W, Bahk J D et al., 2007c. Physiological and protein profiles alternation of germinating rice seedlings exposed to acute cadmium toxicity. *Comptes Rendus Biologies*, 330(10): 735–746.

Ahsan N, Lee D G, Lee K W Alam I, Lee S H, Bahk J D et al., 2008. Glyphosate-induced oxidative stress in rice leaves revealed by proteomic approach. *Plant Physiology and Biochemistry*, 46(12): 1062–1070.

Ahsan N, Lee D G, Kim K H, Alam I, Lee S H, Lee K W et al., 2010. Analysis of arsenic stress-induced differentially expressed proteins in rice leaves by two-dimensional gel electrophoresis coupled with mass spectrometry. *Chemosphere*, 78(3): 224–231.

Alam I, Lee D G, Kim K H, Park C H, Sharmin S A, Lee H et al., 2010. Proteome analysis of soybean roots under waterlogging stress at an early vegetative stage. *Journal of Biosciences*, 35(1): 49–62.

de Deus Barbosa Anjos A E, da Rocha F R, de Lima e Souza D D S, Freire E, de Oliveira N O B et al., 2009. Differentially expressed genes in cotton plant genotypes infected with *Meloidogyne incognita*. *Plant Science*, 177(5): 492–497.

Bradford M M, 1976. A rapid and sensitive method for the quantitation of microgram quantities of protein utilizing the principle of protein-dye binding. *Analytical Biochemistry*, 72(1-2): 248–254.

Castro A J, Carapito C, Zorn N, Magn C, Leize E, Van Dorsselaer A et al., 2005. Proteomic analysis of grapevine (*Vitis vinifera* L.) tissues subjected to herbicide stress. *Journal of Experimental Botany*, 56(421): 2783–2795.

Chen J W, Dodia C, Feinstein S I, Jain M K, Fisher A B, 2000. 1-Cys peroxiredoxin, a bifunctional enzyme with glutathione peroxidase and phospholipase A$_2$ activities. *Journal of Biological Chemistry*, 275(37): 28421–28427.

Cummins I, Cole D J, Edwards R, 1999. A role for glutathione transferases functioning as glutathione peroxidases in resistance to multiple herbicides in black-grass. *The Plant Journal*, 18(3): 285–292.

Davies E J, 2003. Molecular and biochemical characterization of cytosolic phosphoglucomutase in wheat endosperm (*Triticum aestivum* L. cv. Axona). *Journal of Experimental Botany*, 54(386): 1351–1360.

Du C X, Fan H F, Guo S R, Tezuka T, Li J, 2010. Proteomic analysis of cucumber seedling roots subjected to salt stress. *Phytochemistry*, 71(13): 1450–1459.

Fan W H, Cui W T, Li X F, Chen S Y, Liu G S, Shen S H, 2010. Proteomics analysis of rice seedling responses to ovine saliva. *Journal of Plant Physiology*, 168(5): 500–509.

Fanous A, Weiland F, Lück C, Görg A, Friess A, Parlar H, 2007. A proteome analysis of *Corynebacterium glutamicum* after exposure to the herbicide 2,4-dichlorophenoxy acetic acid (2,4-D). *Chemosphere*, 69(1): 25–31.

Gallardo K, Job C, Groot S P, Puype M, Demol H, Vandekerckhove J et al., 2001. Proteomic analysis of Arabidopsis seed germination and priming. *Plant Physiology*, 126(2): 835–848.

Ge R C, Chen G P, Zhao B C, Shen Y Z, Huang Z J, 2007. Cloning and functional characterization of a wheat serine/threonine kinase gene (TaSTK) related to salt-resistance. *Plant Science*, 173(1): 55–60.

Giannakou I O, Karpouzas D G, Anastasiades I, Tsiropoulos N G, Georgiadou A, 2005. Factors affecting the efficacy of non-fumigant nematicides for controlling root-knot nematodes. *Pest Management Science*, 61(10): 961–972.

Guzmangonzalez S, Orozco-Santos M, Farias-Larios L, 1994. Effect of fosthiazate on control of *Radopholus-similis* in banana. *Nematropica*, 24(2s): 165–168.

Hafez S L, Sundararaj P, 2006. Evaluation of fumigant and non-fumigant nematicides for the control of *Meloidogyne chitwoodi* on patato. *Nematollogia Mediterranea*, 34(2): 147–149.

Hashiguchi A, Ahsan N, Komatsu S, 2010. Proteomics application of crops in the context of climatic changes. *Food Research International*, 43(7): 1803–1813.

Hirano H, Harashima H, Shinmyo A, Sekine M, 2008. Arabidopsis retinoblastoma-related protein 1 is involved in G1 phase cell cycle arrest caused by sucrose starvation. *Plant Molecular Biology*, 66(3): 259–275.

Irar S, Brini F, Goday A, Masmoudi K, Pages M, 2010. Proteomic analysis of wheat embryos with 2-DE and liquid-phase chromatography (ProteomeLab PF-2D) – a wider perspective of the proteome. *Journal of Proteomics*, 73(9): 1707–1721.

Jin C X, Liu J J, Bao L L, Zhou Q X, Zhou Q X, 2010. Joint toxicity of sulfamonomethoxine and Cd on seed germination and root elongation of crops in soil. *China Environmental Science*, 30(6): 839–844.

Kim Y K, Lee M Y, 2009. Proteomic analysis of differentially expressed proteins of rice in response to cadmium. *Journal of the Korean Society for Applied Biological Chemistry*, 52(5): 428–436.

Kimpinski J, Arsenault W J, Sanderson J B, 1997. Fosthiazate for suppression of *Pratylenchus penetrans* in potato on Prince Edward Island. *Journal of Nematology*, 29(4S): 685–689.

Kimpinski J, Martin R A, Sturz A V, 2005. Nematicides increase grain yields in spring wheat cultivars and suppress plant-parasitic and bacterial-feeding nematodes. *Journal of Nematology*, 37(4): 473–476.

Kipreos E T, Pagano M, 2000. The F-box protein family. *Genome Biology and Evolution*, 1(5): 1–7.

Kong F J, Oyanagi A, Komatsu S, 2010. Cell wall proteome of wheat roots under flooding stress using gel-based and LC MS/MS-based proteomics approaches. *Biochimica et Biophysica Acta*, 1804(1): 124–136.

Kungolos A, Emmanouil C, Tsiridis V, Tsiropoulos N, 2009. Evaluation of toxic and interactive toxic effects of three agrochemicals and copper using a battery of microbiotests. *Science of the Total Environment*, 407(16): 4610–4615.

Lee D G, Ahsan N, Lee S H, Lee J J, Bahk J D, Kang K Y et al., 2009. Chilling stress-induced proteomic changes in rice roots. *Journal of Plant Physiology*, 166(1): 1–11.

Lee G J, Vierling E, 2000. A small heat shock protein cooperates with heat shock protein 70 systems to reactivate a heat-denatured protein. *Plant Physiology*, 122(1): 189–198.

Li D, Liu H, Zhang H, Wang X, Song F, 2008. OsBIRH1, a DEAD-box RNA helicase with functions in modulating defence responses against pathogen infection and oxidative stress. *Journal of Experimental Botany*, 59(8): 2133–2146.

Lin Y Z, Chen H Y, Kao R, Chang S P, Chang S J, Lai E M, 2008. Proteomic analysis of rice defense response induced by probenazole. *Phytochemistry*, 69(3): 715–728.

Lu T C, Meng L B, Yang C P, Liu G F, Liu G J, Ma W et al., 2008. A shotgun phosphoproteomics analysis of embryos in germinated maize seeds. *Planta*, 228(6): 1029–1041.

Mironov V, de Veylder L, van Montagu M, Inze D, 1999. Cyclin-dependent kinases and cell division in plants-the nexus. *The Plant Cell*, 11(4): 509–522.

Mou Z, Wang X, Fu Z, Dai Y, Han C, Ouyang J, 2002. Silencing of phosphoethanolamine N-methyltransferase results in temperature-sensitive male sterility and salt hypersensitivity in Arabidopsis. *The Plant Cell Online*, 14(9): 2031–2043.

Lee J, Bricker T M, Lefevre M, Pinson S R, Oard J H, 2006. Proteomic and genetic approaches to identifying defence-related proteins in rice challenged with the fungal pathogen *Rhizoctonia solani*. *Molecular Plant Pathology*, 7(5): 405–416.

Okanami M, Meshi T, Iwabuchi M, 1998. Characterization of a DEAD box ATPase/RNA helicase protein of *Arabidopsis thaliana*. *Nucleic Acids Research*, 26(11): 2638–2643.

Palavalli L H, Brendza K M, Haakenson W, Cahoon R E, McLaird M, Hicks L M et al., 2006. Defining the role of phosphomethylethanolamine N-methyltransferase from *Caenorhabditis elegans* in phosphocholine biosynthesis by biochemical and kinetic analysis. *Biochemistry*, 45(19): 6056–6065.

Pantelelis I, Karpouzas D G, Menkissoglu-Spiroudi U, Tsiropoulos N, 2006. Influence of soil physicochemical and biological properties on the degradation and adsorption of the nematicide fosthiazate. *Journal of Agricutural and Food Chemistry*, 54(18): 6783–6789.

Qin S J, Gan J Y, Liu W P, Becker J O, 2004. Degradation and adsorption of fosthiazate in soil. *Journal of Agricutural and Food Chemistry*, 52(20): 6239–6242.

Qureshi M I, Qadir S, Zolla L, 2007. Proteomics-based dissection of stress-responsive pathways in plants. *Journal of Plant Physiology*, 164(10): 1239–1260.

Radchuk V V, Sreenivasulu N, Blume Y, Weschke W, 2007. Distinct tubulin genes are differentially expressed during barley grain development. *Physiologia Plantarum*, 131(4): 571–580.

Requejo R, Tena M, 2005. Proteome analysis of maize roots reveals that oxidative stress is a main contributing factor to plant arsenic toxicity. *Phytochemistry*, 66(13): 1519–1528.

Riechers D E, Kreuz K, Zhang Q, 2010. Detoxification without intoxication: herbicide safeners activate plant defense gene expression. *Plant Physiology*, 153(1): 3–13.

Schröder J, Stenger H, Wernicke W, 2001. α-Tubulin genes are differentially expressed during leaf cell development in barley (*Hordeum vulgare* L.). *Plant Molecular Biology*, 45(6): 723–730.

Schuppler U, He P H, John P C L, Munns R, 1998. Effect of water stress on cell division and cdc 2-like cell-cycle kinase activity in wheat leaves. *Plant Physiology*, 117(2): 667–678.

Shcherban T Y, Shi J, Durachko D M, Guiltinan M J, McQueen-Mason S J, Shieh M et al., 1995. Molecular cloning and sequence analysis of expansins – a highly conserved, multi-gene family of proteins that mediate cell wall extension in plants. *Proceedings of the National Academy of Sciences of the United States of America*, 92(20): 9245–9249.

Song N H, Yin X L, Chen G F, Yang H, 2007. Biological responses of wheat (*Triticum aestivum*) plants to the herbicide chlorotoluron in soils. *Chemosphere*, 68(9): 1779–1787.

Squier T C, 2006. Redox modulation of cellular metabolism through targeted degradation of signaling proteins by the proteasome. *Antioxidants & Redox Signaling*, 8(1-2): 217–228.

Sun W, Van Montagu M, Verbruggen N, 2002. Small heat shock proteins and stress tolerance in plants. *Biochimica et Biophysica Acta*, 1577(1): 1–9.

Tang J, Liu L X, Huang X L, Li Y Y, Chen Y P, Chen J, 2010. Proteomic analysis of *Trichoderma atroviride* mycelia stressed by organophosphate pesticide dichlorvos. *Canadian Journal of Microbiology*, 56(2): 121–127.

Teixeira J, Pereira S, Queiros F, Fidalgo F, 2006. Specific roles of potato glutamine synthetase isoenzymes in callus tissue grown under salinity: molecular and biochemical responses. *Plant Cell, Tissue and Organ Culture*, 87(1): 1–7.

Wang M E, Zhou Q X, 2005. Single and joint toxicity of chlorimuron-ethyl, cadmium, and copper acting on wheat *Triticum aestivum*. *Ecotoxicology and Environmental Safety*, 60(2): 169–175.

Wang W X, Vinocur B, Shoseyov O, Altman A, 2004. Role of plant heat-shock proteins and molecular chaperones in the abiotic stress response. *Trends in Plant Science*, 9(5): 244–252.

Woods S R, Haydock P P J, Edmunds C, 1999. Mode of action of fosthiazate used for the control of the potato cyst nematode *Globodera pallida*. *Annals of Applied Biology*, 135(1): 409–415.

Xu Z Q, Zhou Q X, Liu W T, 2009. Joint effects of cadmium and lead on seedlings of four Chinese cabbage cultivars in northeastern China. *Journal of Environmental Sciences*, 21(11): 1598–1606.

Yan S P, Tang Z C, Su W A, Sun W N, 2005. Proteomic analysis of salt stress-responsive proteins in rice root. *Proteomics*, 5(1): 235–244.

Yang P F, Li X J, Wang X Q, Chen H, Chen F, Shen S H, 2007. Proteomic analysis of rice (*Oryza sativa*) seeds during germination. *Proteomics*, 7(18): 3358–3368.
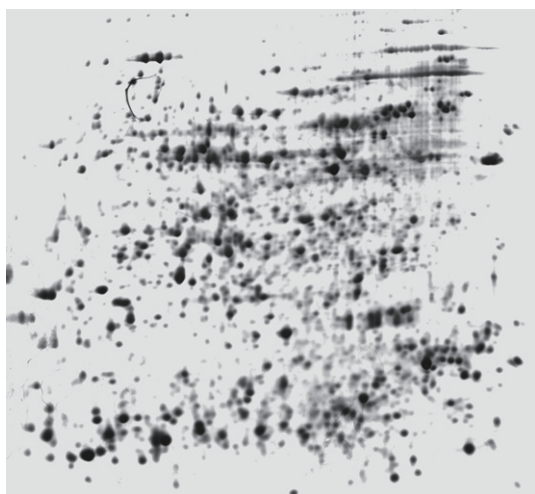
Supporting materials

Three independent replicate protein gels.
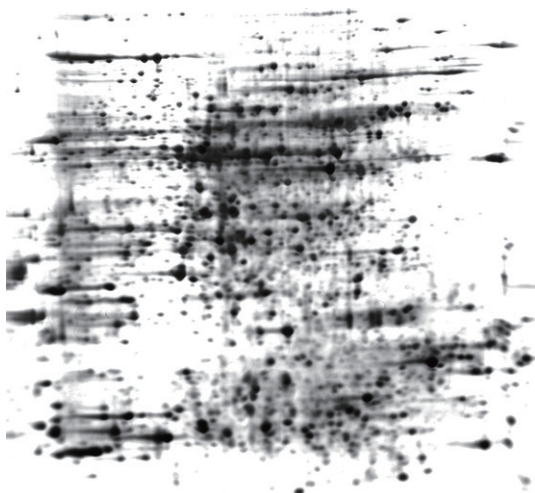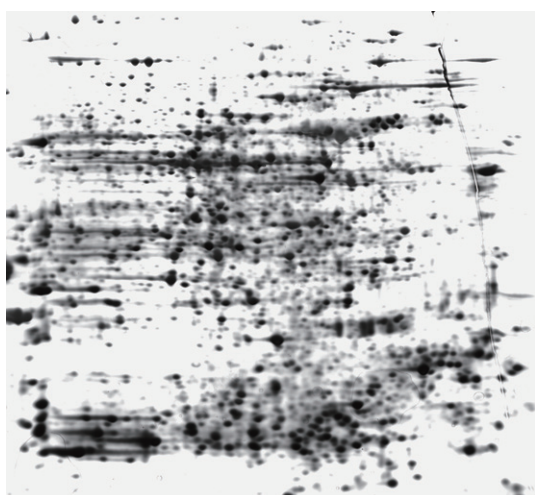

Control-1
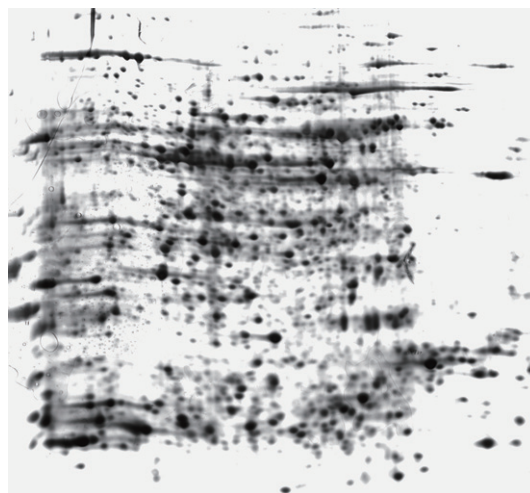
Control-2

Control-3

Fosthiazate-treated-1

Fosthiazate-treated-2

Fosthiazate-treated-3